

A Model for Binding of Structurally Diverse Natural Product Inhibitors of Protein Phosphatases PP1 and PP2A

Varsha Gupta,[†] Anthony K. Ogawa,[†] Xiaohui Du,[†] K. N. Houk, and Robert W. Armstrong*

Department of Chemistry and Biochemistry, University of California, Los Angeles, California 90095

Received December 26, 1996[⊗]

Protein phosphatases play significant roles in signal transduction pathways pertaining to cell proliferation, gene expression, and neurotransmission. Serine/threonine phosphatases PP1 and PP2A, which are closely related in primary structure (~50%), are inhibited by a structurally diverse group of natural toxins. As part of our study toward understanding the mechanism of inhibition displayed by these toxins, we have developed research in two directions: (1) The standardization of an assay to be used in acquisition of the structure–activity relationship of inhibition data is reported. This nonradioactive assay affords detection levels of molecular phosphate released from a phosphorylated hexapeptide in subnanomolar quantities. The comparison of our IC₅₀ values of these inhibitors against corresponding literature data provided validation for our method. (2) Computational analysis provided a global model for binding of these inhibitors to PP1. The natural toxins were shown to possess remarkably similar three-dimensional motifs upon superimposition and van der Waals minimization within the PP1 active site.

Introduction

Endogenous phosphorylation plays a significant role in many cellular processes. Recent studies of the signaling events leading to cell proliferation have implicated the role of phosphatases in these pathways.¹ Phosphatases are present in all eukaryotic cells, and their control presents a number of challenges to medicinal chemists.

Serine/threonine phosphatases comprise a unique class of enzymes consisting of four primary subclasses based on their differences in substrate specificity and environmental requirements.¹ Within the serine/threonine phosphatases, protein phosphatases 1 and 2A (PP1 and PP2A, respectively) share sequence identity of both enzyme catalytic subunits (50% for residues 23–292; 43% overall). Perhaps the most interesting link between PP1 and PP2A is their shared sensitivity toward a structurally diverse family of natural products (see Figure 1). Included in this grouping are calyculins,^{2–4} tautomycin,^{5,6} the nodularins,^{7,8} motuporin,⁹ the microcystins,^{8,10,11} and okadaic acid.^{12,13} *In vitro* competition experiments suggest that inhibition of PP1 and PP2A by these natural products is mutually exclusive with respect to the natural substrates in addition to one another.^{6,11b,14} The structural homology of PP1 and PP2A, combined with the apparent common mode of binding shared by the previously mentioned natural products, provides an interesting entry into the study of binding requirements for each enzyme active site.

Knowledge of structure and subsequent correlation to binding function for both PP1 and PP2A would provide a vital link toward understanding signaling events that result in cell proliferation. The crystal structure solved by Kuriyan *et al.* for the cocrystal of microcystin-LR covalently bound to the catalytic subunit of PP1 at residue Cys273 provides a crucial step in this process.¹⁵ Although this finding offers tremendous knowledge regarding the active site of PP1, studies by

MacKintosh *et al.* in which a covalent adduct of microcystin bound at the *N*-methyldehydroalanine (Mdha) retained inhibition capability strongly suggested that the covalent linkage of PP1 and microcystin represents a secondary binding event.¹⁶ In addition, mutagenesis studies by Lee *et al.* show no significant changes between a Cys273Ala mutant and wild-type in terms of specificity toward phosphorylase *a* and IC₅₀ values for the inhibitors microcystin, nodularin, okadaic acid and tautomycin.¹⁷ Despite the excellent efforts in the structural study of PP1, a detailed analysis of the primary binding requirements remains a goal in understanding structure–function relationships for serine/threonine phosphatases, specifically PP1.

The structural analysis of protein phosphatase inhibitors has been an area of extensive study. The NMR-derived conformation of okadaic acid shows strong correlation to the X-ray structure.¹⁸ In addition, the solution structure studied by NMR and molecular dynamics for microcystin-LR bears striking similarities to the PP1-bound inhibitor conformation.¹⁹ The solution structure and molecular dynamics calculations for nodularin very closely resemble those of microcystin-LR in the chemically equivalent segment.²⁰ Substructure solution NMR studies on calyculin A are consistent with the X-ray data.² Enzyme inhibition studies in combination with NMR studies identified the diacid derivative of tautomycin as the active form of the inhibitor.²¹

We propose to combine information gained from structure–activity relationship (SAR) studies with molecular modeling as part of our investigation into the basic requirements for inhibition by the natural products shown in Figure 1. This paper reports preliminary studies of inhibitors of protein phosphatases PP1 and PP2A. Our use of a nonradioactive assay serves to characterize each parent inhibitor with the intent of verifying the previous collective studies^{17a,22} of the known natural product PP1 and PP2A inhibitors.

Guided by the cocrystal structure of PP1 and microcystin-LR, we used computational studies to propose a

[†] These authors contributed equally to this research.

[⊗] Abstract published in *Advance ACS Abstracts*, August 15, 1997.

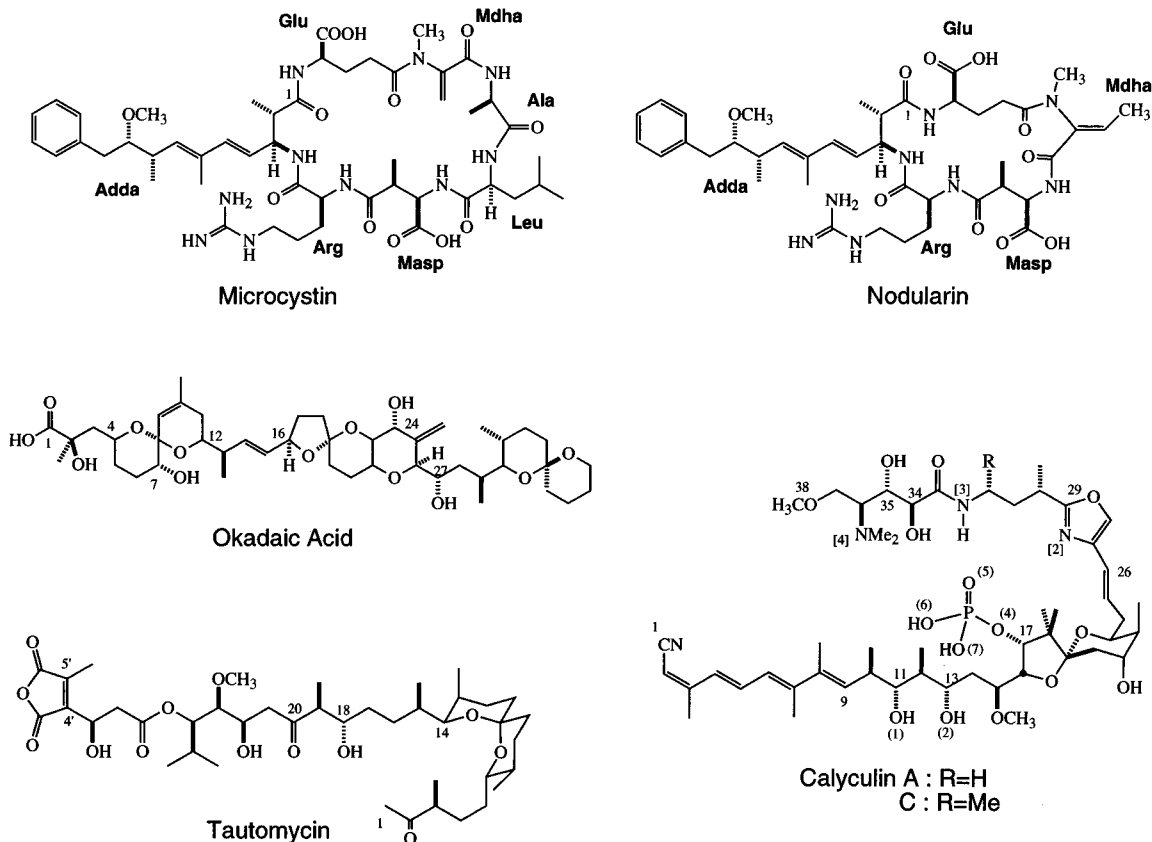


Figure 1. Serine/threonine phosphatase inhibitors. Notation for atom labels: oxygen denoted by parentheses, (x); nitrogen denoted by square brackets, [x].

model for binding of acyclic inhibitors calyculin A and okadaic acid. These studies, in combination with calculations involving microcystin-LR and nodularin, suggest that a macrocyclic structure possessing an aliphatic tail is consistent with an overall mode of binding.

Results and Discussion

Enzyme Assay. As part of our ongoing efforts to study serine/threonine phosphatases, we sought to establish a simple *in vitro* screening method that would allow for future correlation of SAR data. Standardization of activity profiles for tight-binding inhibitors of PP1 and PP2A represented a necessary preface to our SAR study. We report the utilization of an *in vitro* nonradioactive assay that serves as a standard in the acquisition of inhibition data for both PP1 and PP2A.

Selection of the malachite green assay, first reported by Baykov,²³ allowed for quantification of inorganic phosphate *via* the observed absorbance of a the P_i -molybdate-malachite green complex at 650 nm. Our use of a nonradioactive assay obviated the cost associated with radiolabeled peptide substrates while the accuracy of activity determination was maintained. Ekman²⁴ reported a lower limit of P_i detection to be approximately 100 pmol; however, our results showed reliable detection of as little as 20 pmol of P_i (in 30 μ L total volume; see the Supporting Information).

The IC_{50} values for different serine/threonine phosphatase inhibitors from previous experiments vary over a wide concentration range (see Table 1). In addition to variances in assay conditions (temperature and duration, e.g.), differences in the choice of substrate also has an effect on the observed inhibition profiles. A comparison of two common substrates, phosphorylase

Table 1. Inhibition of PP2A by Natural Product Inhibitors^a

inhibitor	IC_{50} (nM)	
	obs	lit.
microcystin	0.065	2–0.04 ^{11,14,22,26,27}
nodularin	0.20	1–0.03 ^{7,22a}
okadaic acid	0.45	1.0–0.02 ^{1c,3,13,14,22,28,29}
tautomycin	10.00	23.1–10 ^{6,14,21,22}
calyculin A	7.30	3–0.25 ^{3,14,17a,22,29,30}
calyculin C	9.71	2.8 ³⁰

^a Error bar <5%.

A (cellular substrate) and *p*-nitrophenol phosphate (*p*NPP), showed that assays using phosphorylase A have better inhibition profiles than *p*NPP, primarily due to a weaker and nonspecific binding of *p*NPP to PP1 and PP2A. Phosphorylase A, however, contains more than one active site, which makes kinetic analysis difficult to interpret. The combination of these factors, in addition to the cost of the desirable more specific substrate, suggested that the use of a simple commercially available phosphopeptide substrate would greatly simplify the assay of phosphatase activity. Pinna *et al.* (multiple studies) and Jirik *et al.* surveyed synthetic phosphopeptides of varying lengths (5mer to 50mer) for their activity as substrates with serine/threonine and tyrosine phosphatases.²⁵ It was shown that phosphothreonine hexapeptides were excellent substrates for serine/threonine phosphatases and possess higher specificity compared to *p*NPP. These observations²⁵ ultimately led to the use of a simple hexapeptide (Lys-Arg-pThr-Ile-Arg-Arg) which was provided by a commercial source (see Experimental Section). Establishment of activity showed the hexapeptide to be >10 times more specific than *p*-nitrophenyl

phosphate.^{13a,14} Our choice of phosphopeptide substrate provided an interesting departure from previous efforts due to its reduced cost and increased availability.

Pertaining to the enzyme assay itself, basic inhibition data supported the earlier findings of Carmichael⁸ and Honkanen^{7,11a} which showed an enzyme concentration dependence of IC₅₀ values for both phosphatases PP1 and PP2A. This observation is characteristic of tight binding enzyme–inhibitor interactions. Optimal concentration values of 1 and 0.1 unit/mL were subsequently established for PP1 and PP2A.

Microcystin-LR and nodularin are cyclic hepta- and pentapeptides structurally unrelated to other serine/threonine phosphatase inhibitors.^{7,8,11} Microcystin-LR is one of the most extensively studied phosphatase inhibitors. However, the IC₅₀ values for microcystins previously reported against PP2A varied from 1 to 0.04 nM, primarily due to the use of different techniques, enzymes concentrations, and/or substrates. Microcystin and nodularin inhibit the activity of PP2A in a dose dependent fashion. The IC₅₀ values for microcystin and nodularin were 0.065 and 0.20 nM (see Figure 2a) with PP2A (3 mU). In contrast to the inhibition of PP2A, the inhibition of PP1 did not display dose dependence with respect to enzyme concentration. The observed IC₅₀ values were 1.17 and 0.42 nM (see Figure 3a) with microcystin-LR and nodularin, respectively. The inhibition curve for microcystin-LR was almost the same as nodularin with both the enzymes.

Okadaic acid and tautomycin are serine/threonine phosphatase inhibitors of the polypropionate class. Although structurally unrelated to microcystin, okadaic acid and tautomycin also showed inhibition of PP2A in a dose dependent manner. Okadaic acid inhibited PP2A with an IC₅₀ of 0.45 nM (see Figure 2b) which was substantially lower than that for tautomycin (IC₅₀ = 10.00 nM). Okadaic acid has been previously used to differentiate between PP2A and other phosphatases due to its high affinity for PP2A. The IC₅₀ of okadaic acid and tautomycin for PP1 were found to be 1.24 and 0.67 nM (see Figure 3b), respectively.

Calyculins A and C are closely related members of the phosphate-bearing class of serine/threonine phosphatase inhibitors.^{2,4} Calyculins were shown to follow similar inhibition curves for the two enzymes (PP1 and PP2A). However, their binding affinity for the two enzymes was different. The IC₅₀ values were 7.30 and 9.71 nM (see Figure 2c) for calyculin A and calyculin C, respectively, against PP2A. These numbers were approximately 2 orders of magnitude higher concentration than that observed for microcystin-LR and okadaic acid. Calyculins A and C (IC₅₀ = 1.20 and 1.49 nM, respectively) were found to be better inhibitors of the enzyme PP1 (see Figure 3c) as compared to okadaic acid.

A central feature of our ongoing efforts toward understanding serine/threonine phosphatases PP1 and PP2A involved the establishment of a reliable method for activity measurement. We feel that the malachite green assay affords general applicability in SAR screening of phosphatase activity. The level of sensitivity achieved (20 pmol of P_i) and overall simplicity affirmed its use in our studies.

Computational Analysis

The binding of microcystin-LR to PP1 was recently determined by the X-ray structure of the inhibitor bound

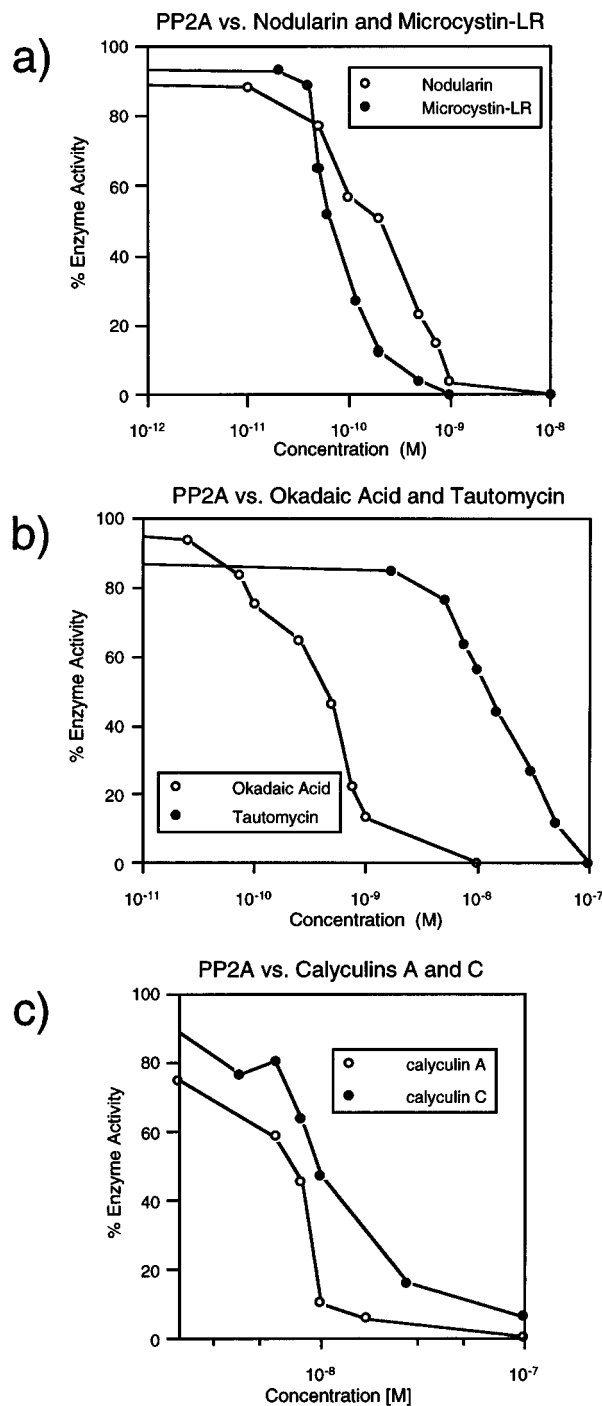


Figure 2. Inhibition profiles against PP2A. The activity of PP2A was assayed in the presence of the indicated amounts of (a) microcystin-LR and nodularin, (b) okadaic acid and tautomycin, and (c) calyculins A and C using phosphopeptide (Lys-Arg-pThr-Ile-Arg-Arg) as substrate.

in the active site of PP1.¹⁵ From this work, three key binding areas of microcystin-LR with PP1 were proposed by Kuriyan *et al.* Atoms in these three regions of microcystin are labeled in Figure 4: (a) the D-erythro- β -methylaspartic acid (Masp) carboxylate hydrogen bonds with Arg96 and Tyr134 of PP1; (b) the Glu carboxylic acid and ADDA carbonyl oxygen hydrogen bond with water molecules that are ligated to either a bivalent cation (presumably Mn²⁺ ion) in the active site or another active site residue; and (c) the ADDA hydrophobic tail extends into the hydrophobic groove

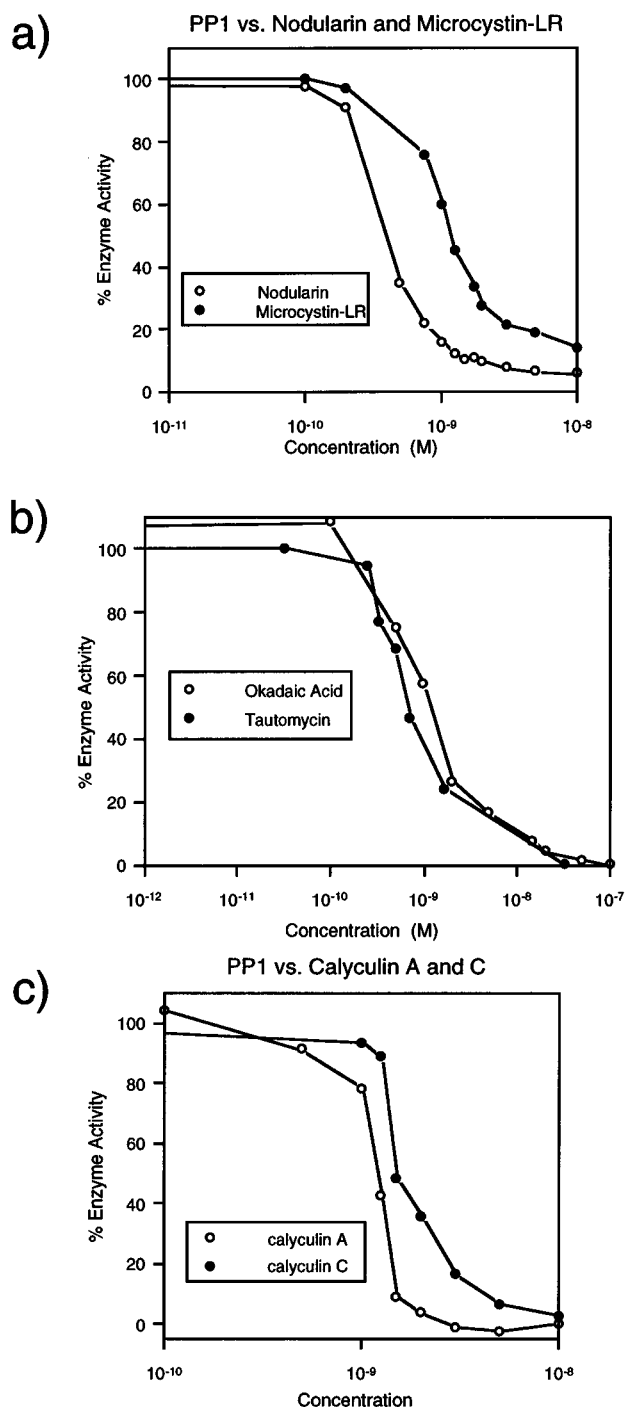


Figure 3. Inhibition profiles against PP1. The activity of PP1 was assayed in the presence of the indicated amounts of (a) microcystin-LR and nodularin, (b) okadaic acid and tautomycin, and (c) calyculins A and C using phosphopeptide (Lys-Arg-pThr-Ile-Arg-Arg) as substrate.

of PP1. The PP1-bound microcystin-LR serves as a template in our modeling of other inhibitors.

In order to model the interactions between other inhibitors and PP1, we first studied conformations of the inhibitors in the gas phase. Gas phase calculations (using AMBER*) and the X-ray conformation of PP1-bound microcystin differ considerably in the conformation of cyclic peptide backbone of the inhibitor. Much reorganization is required for the gas phase conformation of microcystin to achieve the binding conformation found in the PP1 active site. Monte Carlo searches and molecular dynamics calculations involving the inhibitors

show that the "tail" portions (labeled in Figure 4) of each inhibitor are very flexible. Support for this observation lies in the solution NMR and molecular dynamics studies on microcystin and nodularin which report flexibility in the β -(2*S*,3*S*,8*S*,9*S*)-3-amino-9-methoxy-2,6,8-trimethyl-10-phenyldeca-4,6-dienoic acid (ADDA) "tails".^{19,20} These observations would make utilization of gas phase conformations³² problematic in docking studies, since most docking programs either do not permit large changes of ligand conformation or are slow in flexible docking.³³ Indeed, our choice for inhibitor conformations used in docking studies was based on a need for rigidity, and validation of conformational deductions agreed with solution-derived conformations.

The excellent agreement^{12,18,19a} between solution conformations (derived from NMR studies) and X-ray structures of microcystin-LR and okadaic acid supports the use of each inhibitor X-ray structure for docking studies with standard programs. Solution NMR studies show similarity between nodularin and microcystin in their chemically equivalent segment (Masp-Arg-ADDA-Glu).^{19,20} As a consequence, the conformation of nodularin for our docking study was derived from the PP1-bound X-ray conformation of microcystin,¹⁵ optimized with the ADDA "tail" fixed.³⁴ In addition, the X-ray structure of calyculin that was used for our docking study agreed with NMR solution studies on a portion of the calyculin backbone.^{2,12}

We next searched for common components within each of these diverse natural products in order to identify superimposition motifs. Studies by Quinn *et al.* revealed the importance of a cyclic system in modulating binding affinity of microcystin and nodularin.³⁵ Consistent with the implication forwarded by Quinn, the acyclic inhibitors appear to fold onto themselves, resulting in cyclic conformations. This observation is supported by the existence of intramolecular hydrogen bonds between N[3]-H and O(1) in calyculin A² and the C1-carboxylate and C24-hydroxy oxygen in okadaic acid that form 21 and 18-membered pseudo-rings, respectively (from X-ray structures). Furthermore nuclear magnetic resonance studies in solution showed an intramolecular NOE in calyculin C³⁶ between N[3]-H and C9-H atoms which supports the observed cyclic conformation found in the X-ray data. For calyculin, the spiroketal moiety directs the vectors for the bonds involving C25-C26 and C15-C16 in a manner which is consistent with the conformation observed in the Leu-Ala-Mdha residues of microcystin. A similar analysis of okadaic acid suggests that the C4-C12-spiroketal unit is responsible for the effective turn of the molecule. These spirocyclic features reinforce adoption of "circular" conformations despite the acyclic primary structures of okadaic acid and calyculin.

Nodularin, okadaic acid, and calyculin possess three motifs corresponding to the three regions that microcystin uses to interact with PP1. One atom was picked from each region for the best superimposition. Each inhibitor possesses acid motifs (labeled a in Figure 4) that could align with the Masp carboxylic acid group of microcystin. In the vicinity of a basic heteroatom that can form a hydrogen bond (Glu-carboxylate and the ADD-carbonyl in case of microcystin), one adjacent carbon was picked (labeled b in Figure 4) for superimposition. The first atom (labeled c in Figure 4) of the

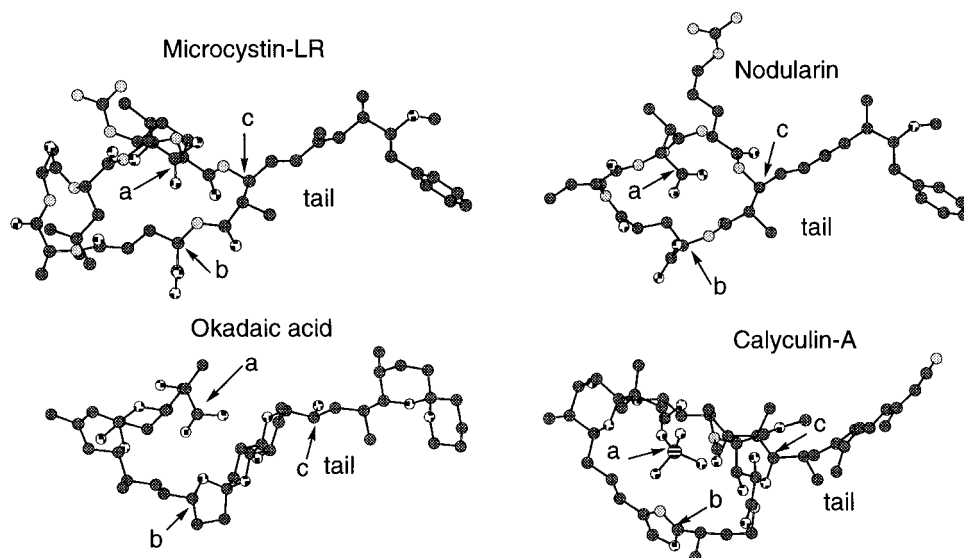


Figure 4. Individual conformations of microcystin-LR, calyculin-A, okadaic acid, and nodularin for superimposition. The atoms for superimposition are shown with arrows: (a) acid functional group, (b) heteroatom region that might interacting with water in inhibitor–enzyme complex, (c) beginning of the hydrophobic tail. See also Table 3 for the detailed atom numbers. The structures are shown according atom type: C: dark shaded; N: light shaded; O: spotted; P: horizontal lined.

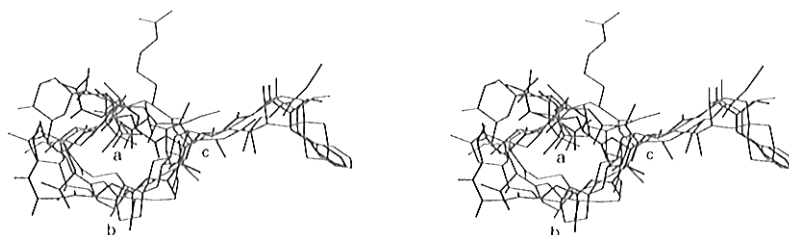


Figure 5. Stereoviews of superimposition of microcystin-LR (blue), nodularin (green), okadaic acid (pink), and calyculin-A (red).

Table 2. Inhibition of PP1 by Natural Product Inhibitors^a

inhibitor	IC ₅₀ (nM)	
	obs	lit.
microcystin	1.17	6.0–0.3 ^{8,10,11,17a,22,27}
nodularin	0.42	3–0.5 ^{7,17a,22a}
okadaic acid	1.24	1300–10 ^{1c,3,13,17a,22,28,29,31}
tautomycin	0.67	7.51–1.1 ^{6,17a,22}
calyculin A	1.20	2.0–0.4 ^{3,17a,22,29,30}
calyculin C	1.49	0.6 ³⁰

^a Error bar <5%.

Table 3. Atom Numbers for Superimposition of the Inhibitors

inhibitor	atom a	atom b	atom c
microcystin-LR	Masp COOH	Glu α-C to N	C3 branched point
nodularin	Masp COOH	Glu α-C to N	C3 branched point
okadaic acid	C1OOH	C16	C27
calyculin-A	OPO(OH) ₂	C29	C11

flexible “tail” that could have van der Waals (VDW) interactions with PP1 was chosen for the overlap. Additionally, the atom labeled c in the case of each inhibitor has an adjacent heteroatom (N or O), which was used as the third atom for overlay.

Remarkable similarities were revealed when nodularin, okadaic acid, and calyculin A were superimposed on the PP1-bound X-ray conformation of microcystin by aligning atoms a, b, and c (see Figure 5 and Table 3).³⁷ The overall root mean square (RMS) deviations correlated with the observed inhibition profiles against PP1 (see Table 1). Given the structural homology between nodularin and microcystin, these structures have the best superimposition. Both terminal ends of the aza-

sugar and tetraene of calyculin qualitatively account for the RMS deviation from the fit, which may be attributed to the differences between its binding conformation and X-ray structure.

Subsequent to this superimposition, we studied optimization to improve favorable VDW and hydrogen-bonding interactions between the inhibitors and PP1.³⁸ There is an attractive VDW interaction (negative interaction energy) between nodularin and PP1. The Masp carboxylic acid group could hydrogen bond with Arg96, and the ADDA side chain fits into the hydrophobic groove as expected (see Figure 6a). The Arg side chain extends out of the active site pocket and presents a flexible component of the molecule. Inspection of the solid state cocrystal structure suggests that this motif is not a key structural component, and therefore should not present a significant problem.

Similar to microcystin, attractive VDW interactions were observed between okadaic acid and PP1. The C1-carboxylic acid could hydrogen bond with Arg96 of PP1. Three hydroxy groups of okadaic acid could also be involved in hydrogen bonding with PP1: the C24-hydroxyl and Arg96; the C27-hydroxyl and Arg221; and the C7-hydroxyl with Glu275. The “tail” section (C27–C37) of okadaic acid fits into the hydrophobic groove very well (see Figure 6b).

For calyculin A (see Figure 6c), optimization of binding in the active site requires noticeable modification of the X-ray structure (*vide supra*). Hydrogen bonds observed in initial docking studies between ca-

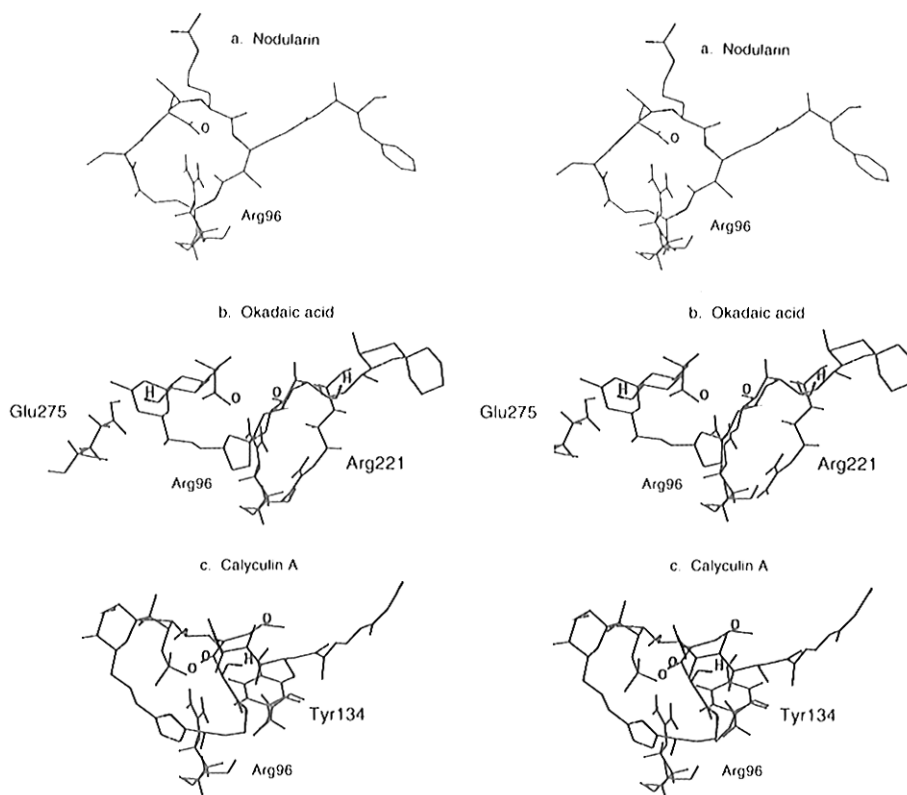


Figure 6. Calculated binding conformations of nodularin (a), okadaic acid (b), and calyculin-A (c) and their possible hydrogen-bonding interactions with PP1. The atoms labeled on the inhibitors are those involved in hydrogen-bonding. The inhibitors are color coded according to atom type: C, green; H, black; N, blue; O, red; P, pink. The active site residues of PP1 involved in hydrogen-bonding interactions are pink.

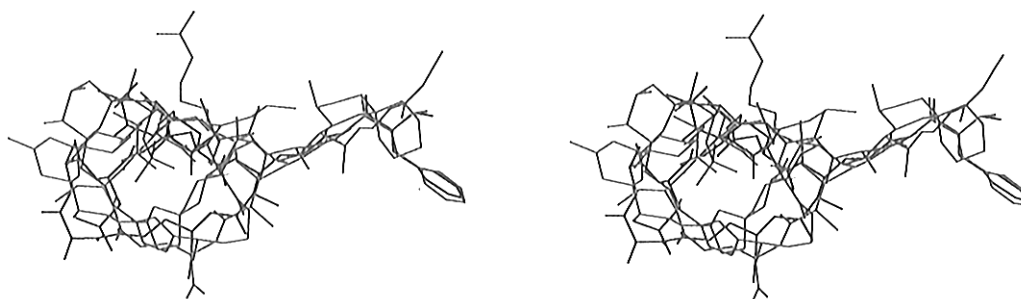


Figure 7. The overlap of microcystin-LR (blue), nodularin (green), okadaic acid (pink), and calyculin-A (red) using PP1 as a reference after minimization of the inhibitors and PP1 complexes.

lyculin A and PP1 include: (1) the C17-phosphate and C35-hydroxyl with Arg96 and (2) the C34-hydroxyl and C37-methoxy group with Tyr134. The poor fit of the C1-C9 tetraene in the hydrophobic groove of PP1 raised the VDW interaction energy in the presence of the aforementioned hydrogen bonding. Minimization of the calyculin A-PP1 complex using a conjugate gradient was performed in an effort to reduce the repulsive VDW interaction of the tetraene. This resulted in the loss of hydrogen bonding between the C17-phosphate and PP1, while the hydrogen bond between the C35-hydroxyl and Arg96 was retained.

Given the discrepancies found in our docking studies involving calyculin A, several questions were raised. Most prominent is the implied role of the C17-phosphate which is presumed to be a key structural component providing organization to the tertiary structure of calyculin through hydrogen bonds between O(5) and O(2)-H, O(7)-H and N[4], and O(6)-H and N[2], thereby reinforcing a circular pattern.² Whether the phosphate

could interact with PP1 without being structurally important remains to be elucidated. One method of investigating the role of C17-phosphate is the synthesis of a C17-desphospho-calyculin analog. Studies to understand the implications presented by the C17-phosphate are currently underway in our group.

The fact that all four inhibitors could interact with Arg96 suggests its importance for binding within the active site. Other orientations were attempted for okadaic acid and calyculin such as superimposing both the C1-carboxylate of okadaic acid and C17-phosphate of calyculin onto the microcystin Glu-carboxylate moiety, but these superimpositions were found to be worse than those described above.

In addition to superimpositions of the four inhibitors using microcystin as a reference, we compared the inhibitors after the VDW minimization of each inhibitor-PP1 complex using PP1 as a spatial template. As shown in Figure 7, there is still a remarkably good overlap of all the inhibitors. This further supports our

hypothesis that, though having diverse structures, the inhibitors might inhibit PP1 with similar three-dimensional structural motifs.

Conclusion

Given the vast interest in serine/threonine phosphatases, a basic understanding of the requirements for binding would provide an important advance and bear implications pertaining to the study of signal transduction. We have reported our initial efforts directed toward establishment of details of the requirements of inhibitor binding. The use of a simple nonradioactive assay provided standardization for inhibition of PP1 and PP2A. A computational study performed on inhibitors calyculin A, nodularin, and okadaic acid has shown remarkably similar three-dimensional motifs upon superimposition. The strong overlap of VDW-optimized inhibitors bound in the PP1-active site supports our model for phosphatase inhibition and serves as the basis for our subsequent SAR study.

Experimental Section

Enzyme Assay. *Reagents.* The enzymes (PP1 and PP2A) and serine/threonine phosphatase assay kit (phosphorylated hexapeptide (Lys-Arg-pThr-Ile-Arg-Arg) and malachite green solutions) were purchased from Upstate Biotechnology, Lake Placid, NY. Calyculin A, microcystin-LR, okadaic acid, and tautomycin were purchased from LC Laboratories, Woburn, MA. Nodularin was purchased from Calbiochem, San Diego, CA. Calyculin C was a generous gift from Professor Nobuhiro Fusetani.

Preparation of Reagents and Buffers. The composition of the enzyme dilution buffer was 20 mM MOPS (pH 7.5), 60 mM 2-mercaptoethanol, 1 mM MgCl₂, and 0.1 mg/mL serum albumin. Dilutions involving substrate were made in distilled deionized water. Initial inhibitor dilutions were made in 1 mL of absolute ethanol, and subsequent dilutions were made in distilled deionized H₂O. The subsequent dilutions of tautomycin were made at pH 8.²¹

The concentration of PP1 used in the assays was 30 mU/well (1 unit of enzyme = ~0.1 μg; 1 unit is defined as the amount required to generate 1 nmol of P_i/min). The concentrations of PP2A used are noted in Figure 2 (1 unit of enzyme = 0.5 μg; 1 nmol of P_i/min). The concentration of substrate stock solution was 0.2 mM for all trials.

General Procedure. Assays were carried out with a reaction time of 60 min at 22 °C. Reactions were initiated by addition of substrate (5 μL) to a mixture containing enzyme (5 μL), buffer (10 μL at indicated pH), and inhibitor (10 μL), thereby affording a total reaction volume of 30 μL/well. Immediately prior to addition of substrate, the enzyme and inhibitor were preincubated for 10 min at the indicated pH. Kinetic experiments conducted in the absence of inhibitor substituted 10 μL of buffer (at indicated pH) for the aforementioned inhibitor aliquot. Assays with PP1 were performed at pH 7.0 (Tris-HCl), while experiments involving PP2A were done at pH 8.0 (Tris-HCl). Reactions were halted via addition of a malachite green solution (50 μL), and UV/vis readings were taken at 650 nm after a 20 min development time. Subsequent plots of inhibition data are representative of a minimum of three trials of each data point.

Computational Methods. The conformations of tautomycin and nodularin were obtained from MacroModel (v 4.5) and Batchmin (v 4.5),³⁹ using the AMBER*⁴⁰ force field. The internal coordinate Monte Carlo protocol developed by Still⁴¹ was used to search for the lowest energy conformation of tautomycin. The GB/SA solvation model⁴² with H₂O as solvent was used for nodularin. The superimpositions of inhibitors and the docking studies were performed with the DISCOVER program (v 2.9.5, Biosym) together with the INSIGHT II (v 2.3.5, Biosym) as a graphic interface. For the docking studies,³³ to reduce computational cost, the water molecules were

deleted from the X-ray structure of PP1, and the PP1 structure was fully constrained when minimizing the energies of the complexes between PP1 and the inhibitors. The complexes between PP1 and inhibitors were minimized using the CVFF force field, with the steepest descent and conjugate gradient algorithms. For nodularin and okadaic acid, the complexes were minimized to a gradient norm of 0.01 kcal/mol Å using a conjugate gradient. For calyculin A, only the steepest descent minimization was employed.

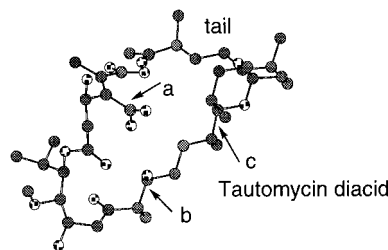
Acknowledgment. We are deeply indebted to Professor Nobuhiro Fusetani for his generous gift of calyculin C. We thank Professor Verne Shoemaker, Ms. Sarada Charugundla, and Dr. Lawrence Castellani for access to the UV/vis plate reader, Professor Yves Rubin for access to his Silicon Graphics workstation, and the Office of Academic Computing for access to an IBM SP-2. We are grateful to Professor John Kuriyan for providing us with the X-ray data of the complex of microcystin and PP1. This work is supported by NIH grant #51095.

Supporting Information Available: Figures reporting substrate specificity and enzyme concentration dependence are provided (3 pages). Ordering information is given on any current masthead page.

References

- (1) For selected review articles, see the following: (a) Wera, S.; Hemmings, B. A. Serine/Threonine Protein Phosphatases. *Biochem. J.* **1995**, *311*, 17–29. (b) Mumby, M. C.; Walter, G. Protein Serine/Threonine Phosphatases: Structure, Regulation and Functions in Cell Growth. *Physiol. Rev.* **1993**, *73*, 673–699. (c) Cohen, P. The Structure and Regulation of Protein Phosphatases. *Annu. Rev. Biochem.* **1989**, *58*, 453–508.
- (2) Kato, Y.; Fusetani, N.; Matsunaga, S.; Hashimoto, K.; Fujita, S.; Furuya, T. Calyculin A, a Novel Antitumor Metabolite from the Marine Sponge, *Discodermia calyx*. *J. Am. Chem. Soc.* **1986**, *108*, 2780–81.
- (3) Ishihara, H.; Martin, B. L.; Brautigan, D. L.; Karaki, H.; Ozaki, H.; Kato, Y.; Fusetani, N.; Watabe, S.; Hashimoto, K.; Uemura, D. Calyculin A and Okadaic Acid: Inhibitors of Protein Phosphatase Activity. *Biochem. Biophys. Res. Commun.* **1989**, *159*, 871–877.
- (4) (a) Kato, Y.; Fusetani, N.; Matsunaga, S.; Hashimoto, K.; Koseki, K. Isolation and Structure Elucidation of Calyculins B, C, and D, Novel Antitumor Metabolites, from the Marine Sponge *Discodermia calyx*. *J. Org. Chem.* **1988**, *53*, 3930–3932. (b) Matsunaga, S.; Fujiki, H.; Sakata, D.; Fusetani, N. Calyculins E, F, G and H, Additional Inhibitors of Protein Phosphatases 1 and 2A from the Marine Sponge *Discodermia calyx*. *Tetrahedron*, **1991**, *47*, 2999–3006.
- (5) Cheng, X. C.; Kihara, T.; Kusakabe, H.; Magae, J.; Kobayashi, Y.; Fang, R. P.; Ni, Z. F.; Shen, Y. C.; Ko, K.; Yamaguchi, I.; Isono, K. A New Antibiotic, Tautomycin. *J. Antibiot.* **1987**, *40*, 907–909.
- (6) MacKintosh, C.; Klumpp, S. Tautomycin from the Bacterium *Streptomyces verticillatus*, Another Potent and Specific Inhibitor of Protein Phosphatases 1 and 2A. *FEBS Lett.* **1990**, *277*, 137–140.
- (7) Honkanen, R. E.; Dukelow, M.; Zwiller, J.; Moore, R. E.; Khatra, B. S.; Boynton, A. L. Cyanobacterial Nodularin is a Potent Inhibitor of Type 1 and Type 2A Protein Phosphatases. *Mol. Pharm.* **1991**, *40*, 577–583.
- (8) An, J.-S.; Carmichael, W. W. Use of a Colorimetric Protein Phosphatase Inhibition Assay and Enzyme Linked Immunosorbent Assay for the Study of Microcystins and Nodularins. *Toxicon* **1994**, *32*, 1494–1507.
- (9) Dilip de Silva, E.; Williams, D. E.; Andersen, R. J.; Klix, H.; Holmes, C. F. B.; Allen, T. M. Motuporin, a Potent Protein Phosphatase Inhibitor Isolated from the Papua New Guinea Sponge *Theonella swinhoei* Gray. *Tetrahedron Lett.* **1992**, *33*, 1561–1564.
- (10) Carmichael, W. W.; Beasley, V.; Bunner, D. L.; Eloff, J. N.; Falconer, I.; Gorham, P.; Harada, K.; Kirshnamurthy, T.; Yu, M.-J.; Moore, R. E.; Rinehart, K. L.; Runnegar, M.; Skulberg, O. M.; Watanabe, M. Naming of Cyclic Heptapeptide Toxins of Cyanobacteria. *Toxicon* **1988**, *26*, 971–973.
- (11) (a) Honkanen, R. E.; Zwiller, J.; Moore, R. E.; Daily, S. L.; Khatra, B. S.; Dukelow, M.; Boynton, A. L. Characterization of Microcystin-LR, a Potent Inhibitor of Type 1 and 2A Protein Phosphatases. *J. Biol. Chem.* **1990**, *265*, 19401–19404. (b)

- MacKintosh, C.; Beattie, K. A.; Klumpp, S.; Cohen, P.; Codd, G. A. Cyanobacterial Microcystin-LR is a Potent and Specific Inhibitor of Protein Phosphatases 1 and 2A from Both Mammals and Higher Plants. *FEBS Lett.* **1990**, *264*, 187–192.
- (12) Tachibana, K.; Scheuer, J.; Tsukitani, Y.; Kikuchi, H.; Van Engen, D.; Clardy, J.; Gopichand, Y.; Schmita, F. J. Okadaic Acid, a Cytotoxic Polyether from Two Marine Sponges of the Genus *Halichondria*. *J. Am. Chem. Soc.* **1981**, *103*, 2469–2471.
- (13) (a) Takai, A.; Mieskes, G. Inhibitory Effect of Okadaic Acid on the *p*-Nitrophenyl Phosphate Activity of Protein Phosphatases. *Biochem. J.* **1991**, *275*, 233–239. (b) Cohen, P.; Klumpp, S.; Schelling, D. L. An Improved Procedure for Identifying and Quantitating Protein Phosphatases in Mammalian Tissues. *FEBS Lett.* **1989**, *250*, 596–600.
- (14) Takai, A.; Sasaki, K.; Nagai, H.; Mieskes, G.; Isobe, M.; Isono, K.; Yasumoto, T. Inhibition of Specific Binding of Okadaic Acid to Protein Phosphatase 2A by Microcystin-LR, Calyculin A and Tautomycin: Method of Analysis of Interactions of Tight-Binding Ligands with Target Protein. *Biochem. J.* **1995**, *306*, 657–665.
- (15) Goldberg, J.; Huang, H.-B.; Kwon, T.-G.; Greengard, P.; Nairn, A. C.; Kuriyan, J. Three-Dimensional Structure of the Catalytic Subunit of Protein Serine/Threonine Phosphatase-1. *Nature* **1995**, *376*, 745–753.
- (16) Moorhead, G.; MacKintosh, R. W.; Morrice, N.; Gallagher, T.; MacKintosh, C. Purification of Type-1 Protein (Serine/Threonine) Phosphatases by Microcystin-Sepharose Affinity Chromatography. *FEBS Lett.* **1994**, *356*, 46–50.
- (17) (a) Zhang, L.; Zhang, Z.; Long, F.; Lee, E. Y. C. Tyrosine-272 is Involved in the Inhibition of Protein Phosphatase-1 by Multiple Toxins. *Biochemistry* **1996**, *33*, 1606–1611. (b) Zhang, Z.; Zhao, S.; Deans-Zirattu, S.; Bai, G.; Lee, E. Y. C. Mutagenesis of the Catalytic Subunit of Rabbit Muscle Protein Phosphatase-1. *Mol. Cell. Biochem.* **1993**, *127*–128, 113–119.
- (18) Matsumori, N.; Murata, M.; Tachibana, K. Conformational Analysis of Natural Products Using Long-Range Carbon-Proton Coupling Constants: Three-Dimensional Structure of Okadaic Acid in Solution. *Tetrahedron* **1995**, *51*, 12229–12238.
- (19) (a) Trogen, G. B.; Annala, A.; Eriksson, J. E.; Konttelt, M.; Meriluoto, J.; Sethson, I.; Zdunek, J.; Edlund, U. Conformational Studies of Microcystin-LR Using NMR Spectroscopy and Molecular Dynamics Calculations. *Biochemistry* **1996**, *35*, 3197–3205. (b) Bagu, J. R.; Sonnichsen, F. D.; Williams, D.; Andersen, R. J.; Sykes, B. D.; Holmes, C. F. B. Comparison of the Solution Structures of Microcystin-LR and Motuporin. *Nature Struct. Biol.* **1995**, *2*, 114–116.
- (20) Annala, A.; Lehtimäki, J.; Mattila, K.; Eriksson, J. E.; Sivonen, K.; Rantala, T. T.; Drakenberg, T. Solution Structure of Nodularin. An Inhibitor of Serine/Threonine-Specific Protein Phosphatases. *J. Biol. Chem.* **1996**, *271*, 16695–16702.
- (21) Sugiyama, Y.; Ohtani, I. I.; Isobe, M.; Takai, A.; Ubukata, M.; Isono, K. Molecular Shape Analysis and Activity of Tautomycin, a Protein Phosphatase Inhibitor. *Bioorg. Med. Chem. Lett.* **1996**, *6*, 3–8.
- (22) (a) Honkanen, R. E. (sp.); Codispoti, B. A.; Tse, K.; Boynton, A. L. Characterization of Natural Toxins with Inhibitory Activity Against Serine/Threonine Protein Phosphatases. *Toxicol.* **1994**, *32*, 339–350. (b) Suganuma, M.; Fujiki, H.; Okabe, S.; Nishiwaki, S.; Brautigan, D.; Ingebritsen, T. S. Structurally Different Members of the Okadaic Acid Class Selectively Inhibit Protein Serine/Threonine But Not Tyrosine Phosphatase Activity. *Toxicol.* **1992**, *30*, 873–878.
- (23) (a) Baykov, A. A.; Evtushenko, O. A.; Aვაeva, S. M. A Malachite Green Procedure for Orthophosphate Determination and its Use in Alkaline Phosphatase-Based Enzyme Assay. *Anal. Biochem.* **1988**, *171*, 266–270. (b) Geladopoulos, T. P.; Sotiroudis, T. G.; Evangelopoulos, A. E. A Malachite Green Colorimetric Assay for Protein Phosphatase Activity. *Anal. Biochem.* **1991**, *192*, 112–116. (c) Ng, D. H. W.; Harder, K. W.; Clark-Lewis, I.; Jirik, F.; Johnson, P. Non-Radioactive Method to Measure CD45 Protein Tyrosine Phosphatase Activity Isolated Directly From Cells. *J. Immunol. Methods* **1994**, *179*, 177–185.
- (24) Ekman, P.; Jager, O. Quantification of Subnanomolar Amounts of Phosphate Bound to Seryl and Threonyl Residues in Phosphoproteins Using Alkaline Hydrolysis and Malachite Green. *Anal. Biochem.* **1993**, *214*, 138–141.
- (25) (a) Pinna, L. A.; Donella-Deana, A. Phosphorylated Synthetic Peptides as Tools for Studying Protein Phosphatases. *Biochim. Biophys. Acta* **1994**, *1222*, 415–431. (b) Donella-Deana, A.; Meyer, H. E.; Pinna, L. A. The Use of Phosphopeptides to Distinguish Between Protein Phosphatase and Acid/Alkaline Phosphatase Activities: Opposite Specificity Toward Phosphoseryl/Phosphothreonyl Substrates. *Biochim. Biophys. Acta* **1991**, *1054*, 130–133. (c) Donella-Deana, A.; MacGowan, C. H.; Cohen, P.; Marchiori, F.; Meyer, H. E.; Pinna, L. A. An Investigation of the Substrate Specificity of Protein Phosphatase 2C Using Synthetic Peptide Substrates; Comparison with Protein Phosphatase 2A. *Biochim. Biophys. Acta* **1990**, *1051*, 199–202. (d) Agostinis, P.; Goris, J.; Pinna, L. A.; Marchiori, F.; Perich, J. W.; Meyer, H. E.; Merlevede, W. Synthetic Peptides as Model Substrates for the Study of the Specificity of the Polycation-Stimulated Protein Phosphatases. *Eur. J. Biochem.* **1990**, *189*, 235–241. (e) Agostinis, P.; Goris, J.; Waelkens, E.; Pinna, L. A.; Marchiori, F.; Merlevede, W. Dephosphorylation of Phosphoproteins and Synthetic Phosphopeptides. *J. Biol. Chem.* **1987**, *262*, 1060–1064. (f) Harder, K. W.; Owen, P.; Wong, L. K. H.; Aebersold, R.; Clark-Lewis, I.; Jirik, F. R. Characterization and Kinetic Analysis of the Intracellular Domain of Human Protein Tyrosine Phosphatase β (HPTP β) Using Synthetic Phosphopeptides. *Biochem. J.* **1994**, *298*, 395–401.
- (26) (a) Matsushima, R.; Yoshizawa, S.; Watanabe, M. F.; Harada, K.-I.; Furusawa, M.; Carmichael, W. W.; Fujiki, H. *In Vitro* and *In Vivo* Effects of Protein Phosphatase Inhibitors, Microcystins and Nodularin, on Mouse Skin and Fibroblasts. *Biochem. Biophys. Res. Commun.* **1990**, *171*, 867–874. (b) Toivola, D. M.; Eriksson, J. E.; Brautigan, D. L. Identification of Protein Phosphatase 2A as the Primary Target for Microcystin-LR in Rat Liver Homogenates. *FEBS Lett.* **1994**, *344*, 175–180.
- (27) Eriksson, J. E.; Toivola, D.; Meriluoto, J. A. O.; Karaki, H.; Han, Y.-G.; Hartshorne, D. Hepatocyte Deformation Induced by Cyanobacterial Toxins Reflects Inhibition of Protein Phosphatases. *Biochem. Biophys. Res. Commun.* **1990**, *173*, 1347–1353.
- (28) Takai, A.; Ohno, Y.; Yasumoto, T.; Mieskes, G. Estimation of the Rate Constants Associated with the Inhibitory Effect of Okadaic acid on Type 2A Protein Phosphatase by Time-Course Analysis. *Biochem. J.* **1992**, *287*, 101–106.
- (29) Gopalakrishna, R.; Chen, Z. H.; Gundimeda, U. Nonphorbol Tumor Promoters Okadaic Acid and Calyculin A Induce Membrane Translocation of Protein Kinase C. *Biochem. Biophys. Res. Commun.* **1992**, *189*, 950–957.
- (30) Fusetani, N.; Matsunaga, S. Bioactive Sponge Peptides. *Chem. Rev.* **1993**, *93*, 1793–1806.
- (31) Murata, K.; Sakon, M.; Kambayashi, J.; Yukawa, M.; Ariyoshi, H.; Shiba, E.; Kawasaki, T.; Kang, J.; Mori, T. The Effects of Okadaic Acid and Calyculin A on Thrombin Induced Platelet Reaction. *Biochem. Int.* **1992**, *26*, 327–334.
- (32) Monte Carlo conformational searches using water as a solvent resulted in excessively flexible conformations.
- (33) For a recent program that allows fast docking of flexible ligands to protein binding sites, see: Welch, W.; Ruppert, J.; Jain, A. N. Hammerhead: Fast, Fully Automated Docking of Flexible Ligands to Protein Binding Sites. *Chem. Biol.* **1996**, *3*, 449–462.
- (34) The lack of an X-ray structure for tautomycin precluded its use in our docking studies. We show only the lowest energy gas phase conformation of the diacid²¹ (see below) for comparison purposes. The labeled atoms in tautomycin are (a) C4'-OOH, (b) C20, and (c) C14.



- (35) Taylor, C.; Quinn, R. J.; Alewood, P. Inhibition of Protein Phosphatase 2A by Cyclic Peptides Modelled on the Microcystin Ring. *Bioorg. Med. Chem. Lett.* **1996**, *6*, 2113–2116.
- (36) ROESY without TOCSY experiments were performed by D. P. Sutherland, J. Strouse, and L. S. Chong. Unpublished results.
- (37) The RMS value for superimposition between nodularin and microcystin is 0.33, between okadaic acid and microcystin is 1.37, and between calyculin and microcystin is 0.94.
- (38) The VDW interaction energy between nodularin and PP1 is –83 kcal/mol, between okadaic acid and PP1 is –52 kcal/mol, between calyculin and PP1 before conjugate gradient minimization is 193 kcal/mol, and after conjugate gradient minimization is –44 kcal/mol.
- (39) Mohamadi, F.; Richards, N. G. J.; Guida, W. C.; Liskamp, R.; Lipton, M.; Caufield, C.; Chang, G.; Hendrickson, T.; Still, W. C. MacroModel—An Integrated Software System for Modeling Organic and Bioorganic Molecules Using Molecular Mechanics. *J. Comput. Chem.* **1990**, *11*, 440–467.
- (40) Weiner, S. J.; Kollman, P. A.; Case, D.; Singh, U. C.; Ghio, C.; Alagona, G.; Profeta, S.; Weiner, P. A New Force Field for Molecular Mechanical Simulation of Nucleic Acids and Proteins. *J. Am. Chem. Soc.* **1984**, *106*, 765–784.
- (41) Chang, G.; Guida, W. C.; Still, W. C. An Internal Coordinate Monte Carlo Method for Searching Conformational Space. *J. Am. Chem. Soc.* **1989**, *111*, 4379–4386.
- (42) Still, W. C.; Tempczyk, A.; Hawley, R. C.; Hendrickson, T. Semianalytical Treatment of Solvation for Molecular Mechanics and Dynamics. *J. Am. Chem. Soc.* **1990**, *112*, 6127–6129.